AD-A107 813 ARMY ARMAMENT RESEARCH AND DEVELOPMENT COMMAND DOVER--ETC F/G 19/1
GUN OPERATED FIRING DEVICE FOR 20-MM AMMUNITION,(U)
NOV 81 R A ZANGRANDO
UNCLASSIFIED ARLCD-MR-81035 SBI-AD-E400 641 NL

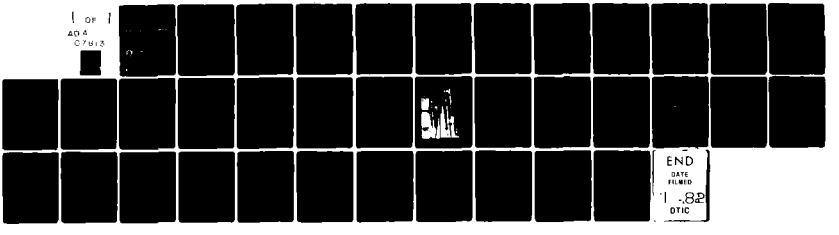

MEMORANDUM REPORT ARLCD-MR-81035

GUN OPERATED FIRING DEVICE FOR 20-mm AMMUNITION

ROY A. ZANGRANDO

NOVEMBER 1981

US ARMY ARMAMENT RESEARCH AND DEVELOPMENT COMMAND
LARGE CALIBER
WEAPON SYSTEMS LABORATORY
DOVER, NEW JERSEY

APPROVED FOR PUBLIC RELEASE; DISTRIBUTION UNLIMITED.

The views, opinions, and/or findings contained in this report are those of the author(s) and should not be construed as an official Department of the Army position, policy, or decision, unless so designated by other documentation.

Destroy this report when no longer needed. Do not return it to the originator.

The citation in this report of the names of commercial firms or commercially available products or services does not constitute official endorsement or approval of such commercial firms, products, or services by the United States Government.

UNCLASSIFIED

SECURITY CLASSIFICATION OF THIS PAGE (When Data Entered)

REPORT DOCUMENTATION PAGE		READ INSTRUCTIONS BEFORE COMPLETING FORM
1. REPORT NUMBER Memorandum Report ARLCD-MR-81035	2. GOVT ACCESSION NO. AD107 813	3. RECIPIENT'S CATALOG NUMBER
4. TITLE (and Subtitle) GUN OPERATED FIRING DEVICE FOR 20-mm AMMUNITION		5. TYPE OF REPORT & PERIOD COVERED 6. PERFORMING ORG. REPORT NUMBER
7. AUTHOR(s) Roy A. Zangrando		8. CONTRACT OR GRANT NUMBER(s)
9. PERFORMING ORGANIZATION NAME AND ADDRESS ARRADCOM, LCWSL Nuclear and Fuze Div (DRDAR-LCN-C) Dover, NJ 07801		10. PROGRAM ELEMENT, PROJECT, TASK AREA & WORK UNIT NUMBERS AH19-TA-G Project Number
11. CONTROLLING OFFICE NAME AND ADDRESS ARRADCOM, TSD STINFO Div (DRDAR-TSS) Dover, NJ 07801		12. REPORT DATE November 1981 13. NUMBER OF PAGES 37
14. MONITORING AGENCY NAME & ADDRESS(if different from Controlling Office) ARRADCOM, SCWSL Armaments Div (DRDAR-SCA) Dover, NJ 07801		15. SECURITY CLASS. (of this report) Unclassified 15a. DECLASSIFICATION/DOWNGRADING SCHEDULE

16. DISTRIBUTION STATEMENT (of this Report)

Approved for public release; distribution unlimited.

17. DISTRIBUTION STATEMENT (of the abstract entered in Block 20, if different from Report)

18. SUPPLEMENTARY NOTES

19. KEY WORDS (Continue on reverse side if necessary and identify by block number)

Firing device
Magnetic
Generator
Electric primer
Machine gun

20. ABSTRACT (Continue on reverse side if necessary and identify by block number)

A new 20-mm infantry machine gun requires a self-contained power source to fire electric-primed ammunition. An exploratory development effort has demonstrated that the motion of the gas-operated weapon can generate electric power sufficient to initiate an M52 primer. This report describes the design considerations, test model, and performance of a permanent magnet firing device used to establish feasibility.

DD FORM 1 JAN 73 1473 EDITION OF 1 NOV 65 IS OBSOLETE

UNCLASSIFIED

SECURITY CLASSIFICATION OF THIS PAGE (When Data Entered)

CONTENTS

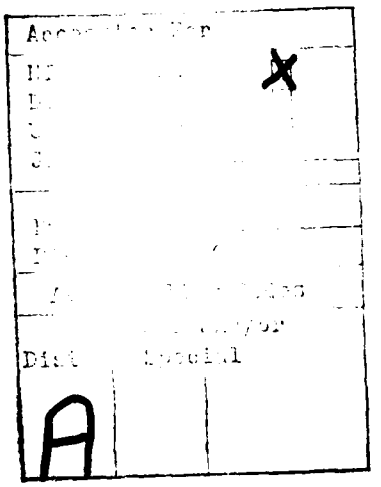

FIGURES

INTRODUCTION

A new 20-mm heavy machine gun which is under development at ARRADCOM is intended to fill an infantry need. A variety of 20-mm tri-service ammunition is available but most types are electric primed and are used in vehicle and aircraft mounted weapons where a source of electric power is available. To take full advantage of this tri-service ammunition, a more convenient source of power must be available. For infantry use, an additional item of equipment would significantly affect the portability, maintenance, and overall operational utility of the weapon. This study demonstrates the feasibility of incorporating a device in the gun which will convert the physical motion of the bolt carrier into electric power sufficient to initiate the primer.

DISCUSSION

Primer Characteristics

The M52A3B1 electric primer is used on all current 20-mm electric-primed ammunition. In lieu of a bridgewire, the primer mix contains a conductive powder and initiation takes place by electrostatic discharge. Because of the nonhomogeneous mixture, the electrical resistance varies from 1000 ohms to 1.2 megaohms with most falling in the higher range. This resistance drops upon application of voltage.

Development experience has shown capacitor discharge to be the best means of initiation. Low DC voltage (24 V dc) will initiate but not reliably, while high voltages (> 180 V dc) may cause arc-over at high altitudes [15,000 m (50,000 ft)]. AC voltage of 440 V at 400 Hz also results in unreliable initiation. MIL-P-1340 which defines the acceptance test methods for this ammunition, calls for all to function with a 10-microsecond discharge from a 2-microfarad capacitor charged to 160 volts. There is no known record of the minimum all-fire energy level. The typical behavior of current and voltage with time during initiation is shown in figure 1.

General Approach

The weapon is gas operated and during operation, the operating group assembly (fig. 2) oscillates fore and aft along the upper receiver tube to: advance the feed, chamber the round, impact the firing pin, and withdraw the spent casing. It is proposed that this oscillatory motion be used to induce voltage in a coil as it passes a permanent magnet. The energy would be stored in a capacitor circuit connected to an insulated firing pin which discharges upon contact with the primer cap. The capacitor would duplicate that specified in the test acceptance criteria to assure an all-fire design. To be self-starting, all the required energy must be generated on the forward stroke.

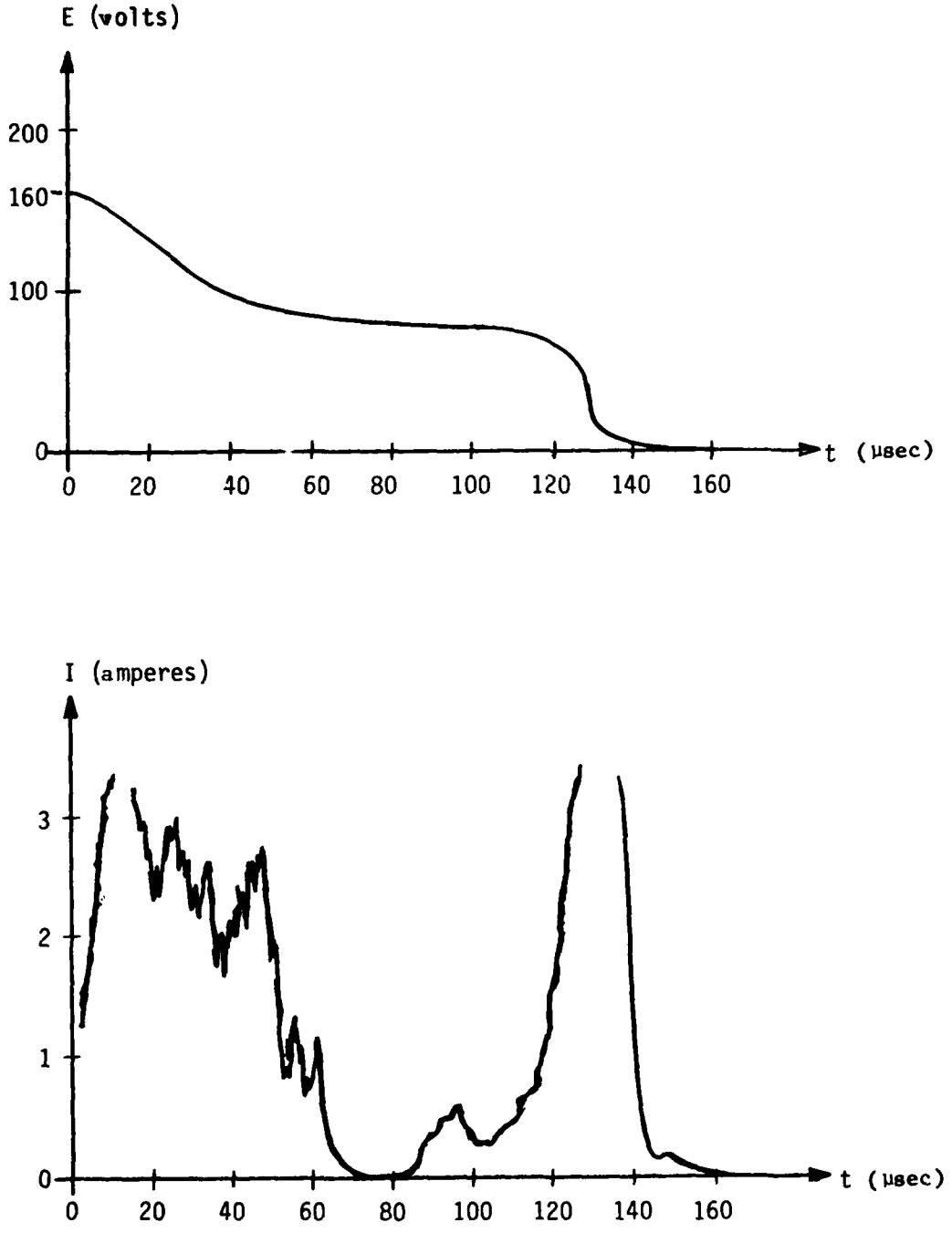

Figure 1. Initiation characteristics of primer

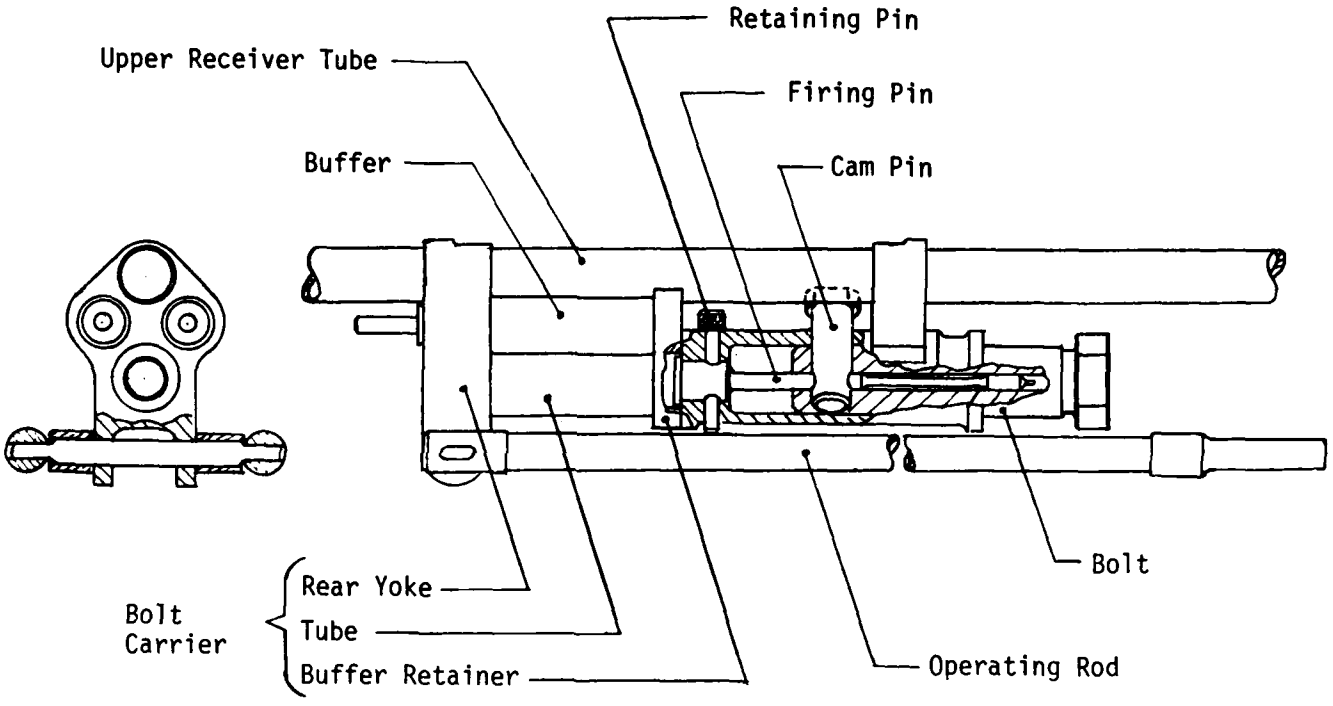

Figure 2. Operating group assembly

Material Selection

The functional requirements of this application suggest desirable characteristics for the demagnetization curve of the permanent magnet. Since the voltage requirement is high (160 V), a high residual flux density, B_r, is probably the most important characteristic. Equally important is the slope of the upper portion of the curve. A square curve is desirable insofar as the loss in flux density due to open circuit and back EMF demagnetization is minimized. For such a curve, the coercive force, H_c, need not be unusually high, as the circuit load will not produce any significant demagnetization. Also, for a square curve, the maximum energy product (B_oH_o) which defines the point of maximum efficiency for that material (max output/unit volume) is high.

The effects of the recoil, however, complicate the matter. The gas pressure returns the bolt carrier at more than three times the speed of the initial stroke and generates a proportionally higher voltage with its associated demagnetizing influence. This phenomenon requires a magnet with a much higher coercive force as well as a high flux density, a combination which is difficult to obtain in common magnet materials. Since the energy obtained on recoil is not usable, a more practical approach would be to eliminate it entirely. Means to open circuit the coil on the return stroke can accomplish this and the magnet can then be designed to the characteristics described above.

Cast Alnico V (fig. 3), a common commercial alloy of Fe, Co, Ni, Al, and Co, meets these characteristics. Other more exotic materials may offer improved characteristics; however, for economic and availability reasons, they should not be used unless necessary. Another feature of Alnico V is its relatively good shock and temperature resistance which enhances its reliability in an automatic weapon.

A yoke completes the magnetic circuit when it is aligned with the magnet. It must be a magnetically soft material with a low residual magnetism and a high initial permeability. A high resistivity minimizes the eddy currents resulting from the AC nature of the pulse. Eddy current losses can further be reduced by constructing the yoke of laminated sheets; however, this is difficult to achieve for the yoke configurations proposed.

There are a variety of electrical core irons on the market. These are special alloys and are difficult to obtain without a special mill run and long lead time. A common inexpensive alternative is low carbon steel such as 1005, 1010, or 1018 which have good magnetic properties suitable for this application. They should be annealed dead soft after all machining.

Configuration

The firing device components must be divided between the operating group assembly and a stationary part of the gun to achieve relative motion. To assure a practical means of electrical connection, the coil and firing circuit should be part of the operating group assembly with the firing pin. Furthermore, placement of the coil on the yoke rather than on the magnet will produce the greater flux change by minimizing the amount of leakage flux linking the coil.

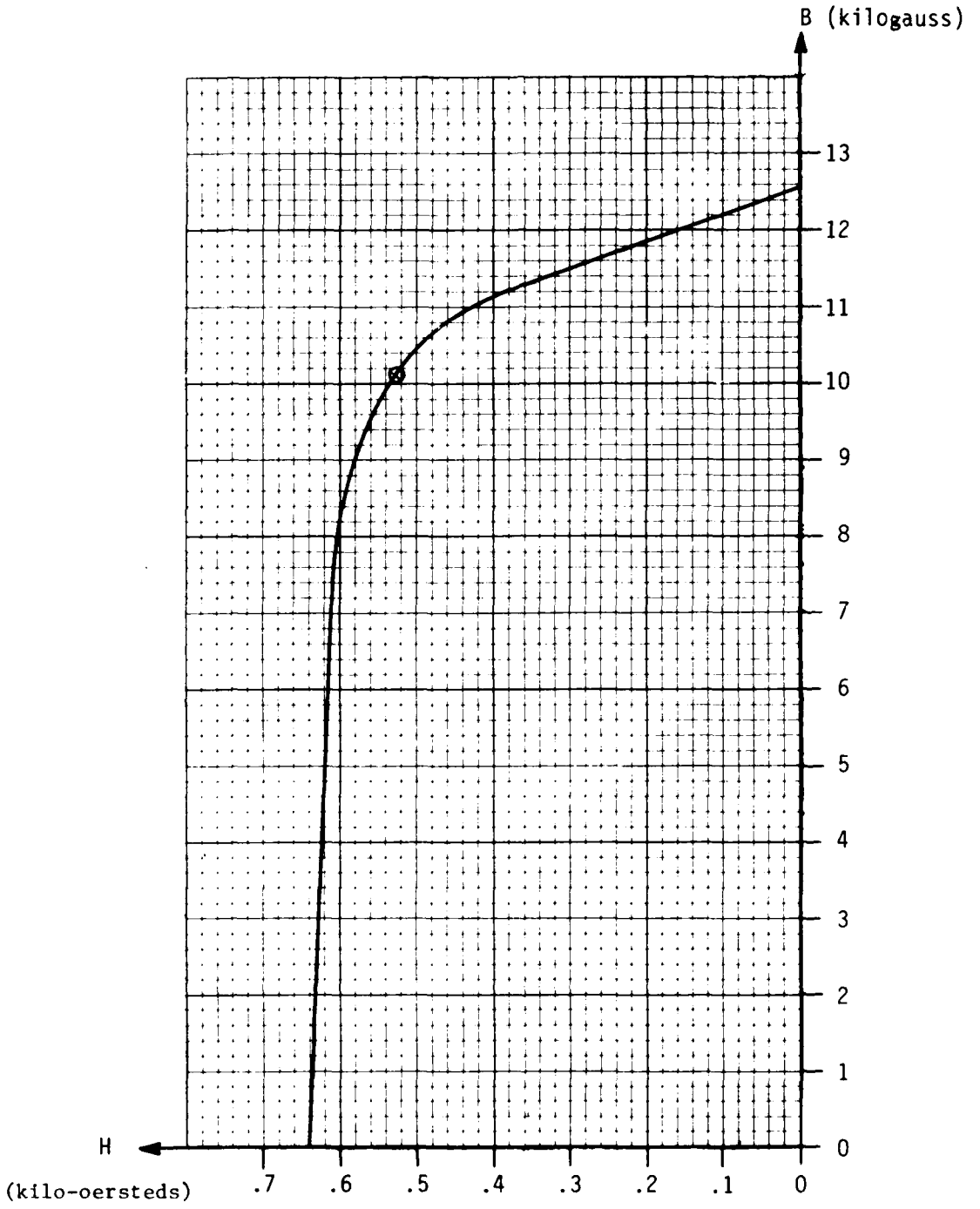

Figure 3. Demagnetization curve for Alnico V

Higher voltages can be achieved with long thin magnets because they have less open circuit demagnetization than short wide magnets of equal volume. Considering the dimensional aspects of the gun, it is likely that a long magnet would have to be positioned longitudinally.

High flux changes can be produced by impacting an armature into the magnet or by withdrawing it from the armatures equally as fast. The key feature here is the zero air gap. This method has been successful on one-shot items; however, since impact destroys magnetic properties this method is not suitable. The yoke must therefore pass by the magnet in a manner which avoids physical contact yet minimizes the air gap. Considering the positional tolerance variations between the moving and stationary parts it would be appropriate to guide the yoke into the proper alignment.

The design configurations chosen for study are illustrated in figure 4. The relationship of the upper receiver tube to the bolt carrier makes the tube a suitable location for the magnet, and this will conveniently serve as a guide for the yoke. A bar magnet is housed within a nonmagnetic receiver tube with magnetic iron pole pieces to pass the magnetic field through the tube. Cast magnets should be centerless ground to assure a good fit in the tube.

Two yoke configurations were tested. The primary approach was a concentric design in which the coil is housed in a cylindrical yoke which surrounds the magnet. When this yoke passes over the magnet, the entire leakage flux is linked to the coil and is only augmented by the yoke. The yoke material thereby becomes less significant.

For comparison, a horseshoe yoke was tested. In this design, the flux linking the coil is routed primarily through the yoke causing the magnetic properties of the yoke to become more important.

Generator Design

The 2 microfarad capacitor defined in the acceptance specification requires an energy input of 0.025 joules to attain full charge. This is a significant energy level which suggests a large magnet. For the configuration chosen in this design, the size of the magnet is constrained by the I.D. of the upper receiver tube (1.0 in.) and the stroke of the bolt carrier (approximately 9 in.).

The general relationship of voltage output to stroke is shown in figure 5. The magnet length is thus limited to 1/2 of the stroke if only the positive (or negative) pulse is used and 1/3 of the stroke if both are used. Both approaches have peculiar benefits and problems. For initial testing, the magnet chosen was 1 in. diameter by 3 in. long.

Trial calculations for this configuration of the demagnetization curve for Alnico V (app A, fig. 6) can be interpreted as follows:

Referring to the general curve at the top, the residual flux density (Br) is that remaining in the material after the magnetizing field has been removed.

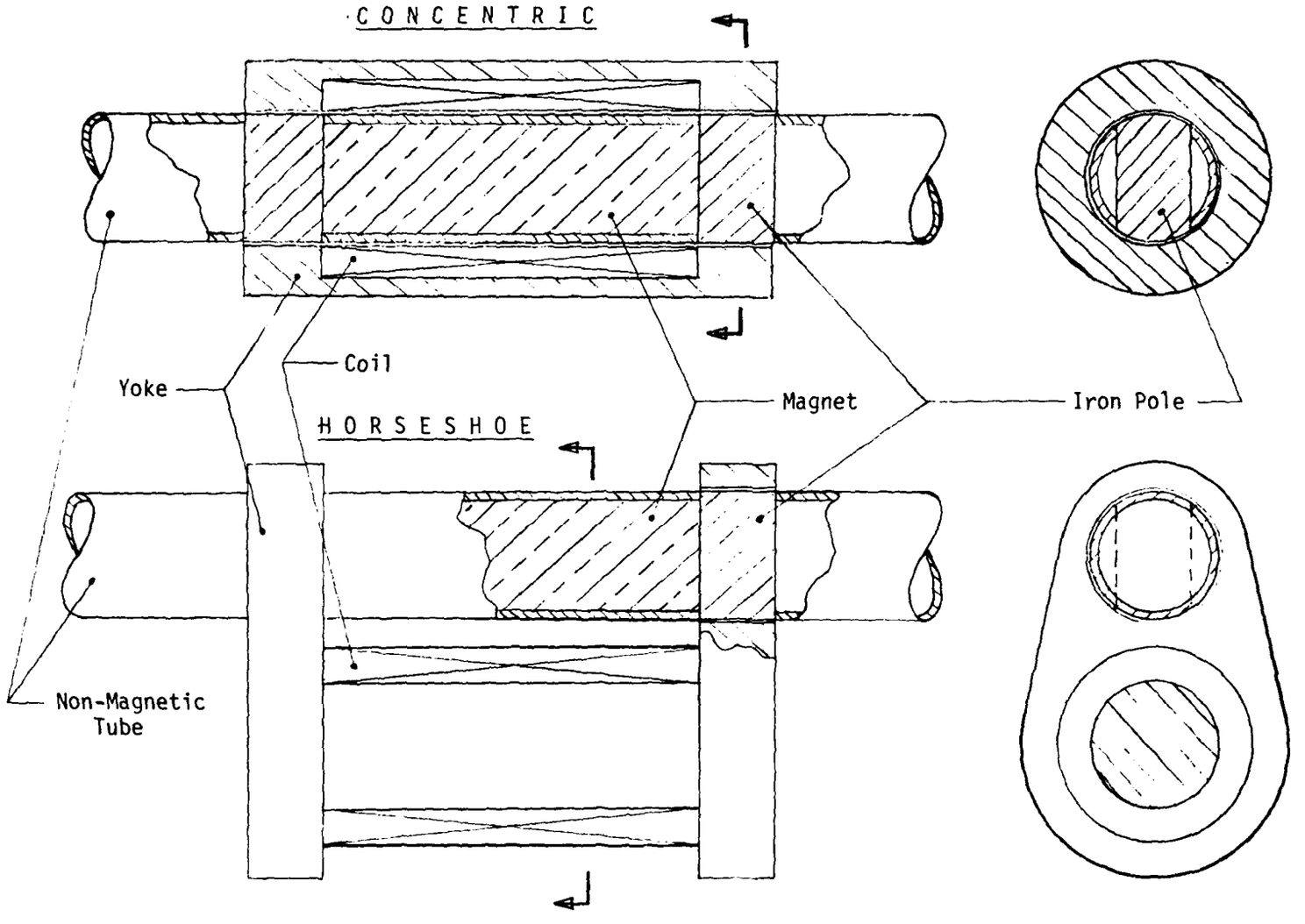

Figure 4. Test configurations

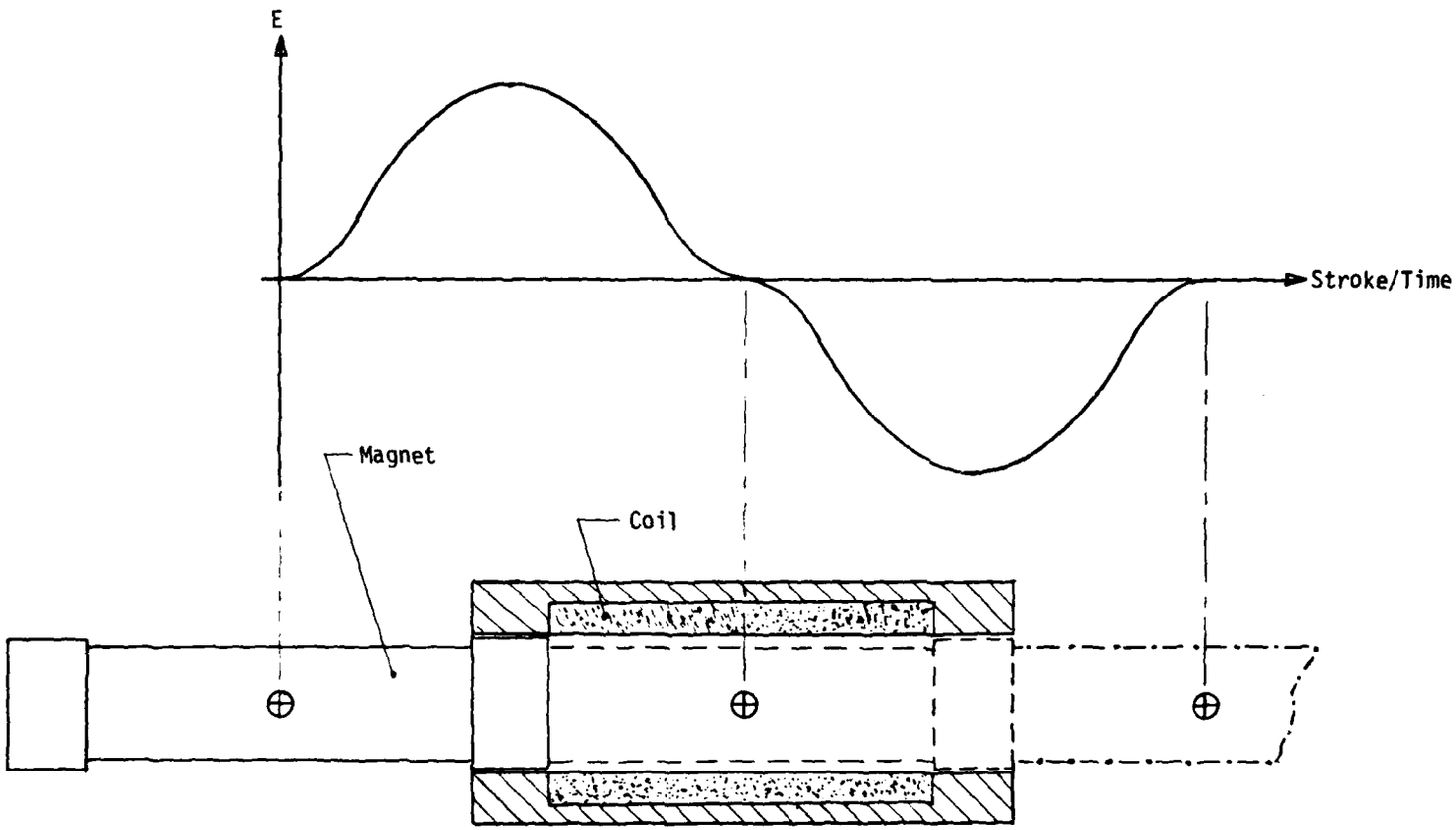

Figure 5. Relationship of voltage output to stroke

Removal of the keeper causes the operating point to move down the curve to the open circuit point, B_pH_p, whereupon subsequent replacement will cause the point to return, not along the original curve but rather along a minor hysterisis loop to x. After several cycles, the magnet stabilizes on this path which can be approximated by a straight line almost parallel to the upper portion of the curve. For maximum efficiency, it is desirable to operate as close as possible to B_0B_0.

When the magnet is aligned with the yoke, the latter serves the function of a keeper but with an air gap. The effects of this gap are shown in figure 6 by the air gap line which leaves the operating point at B_tH_t rather than at x.

During operation, the inductive effect of the coil creates a magnetic field, H_d, opposing that of the magnet. This demagnetizing influence forces the operating point further down the minor hysterisis loop to B_fB_f, which is the final operating point. Should H_D be larger than H_p, the operating point would continue down the demagnetization curve and return along a new minor hysterisis loop lower than the first with an accompanying decreasein B_f, thus decreasing the strength of the magnet.

Calculations were performed for both 3- and 4-inch magnets. In addition, the effect of the large air gap created by omission of the pole pieces was also investigated.

Using the 3-in. magnet, B_pB_p is approximately equal to the maximum energy product B_0B_0 which is an ideal situation. Because of the flatness of the curve, the large increase in air gap resulting from elimination of the pole pieces (0.030 in. to 0.250 in.) causes only a small decrease in flux density. Provided the proper voltage level can be achieved, the larger gap is preferable because it reduces the complexity of the assembly and the high friction drag which occurs with mutual attraction of the pole and the yoke when they are adjacent.

As one might expect, the 4-in. magnet produces a higher output. The narrowness of the curve at these higher levels creates a marginal situation for the large gap configuration. With the final operating point coincident with B_pH_p, any increase in the speed of the bolt carrier beyond that used in the calculations (9 ms per in.) would have the permanent demagnetizing effect described above. On the other hand, it would then become more stabilized and more resistant to further demagnetization.

The longitudinal orientation of the magnet results in a pulse width sufficiently long relative to the time constant of the capacitor circuit. Thus, there is little risk of not achieving a full charge.

The number of turns of wire necessary to generate the required voltage leads to the conclusion that both the positive and negative pulse, rather than only one, should be used. Calculations indicate that the number of turns required to achieve a single 160-volt pulse (15000) are difficult to fit in the intended space. Furthermore, the demagnetization (H_d) effects of that many turns may result in a permanent demagnetizing effect if larger air gaps are used. For this configuration, current flow on the return stroke can be eliminated only by physically breaking the circuit with a switch. Such a switch can be functioned inertially, thus taking advantage of the high acceleration of the return stroke.

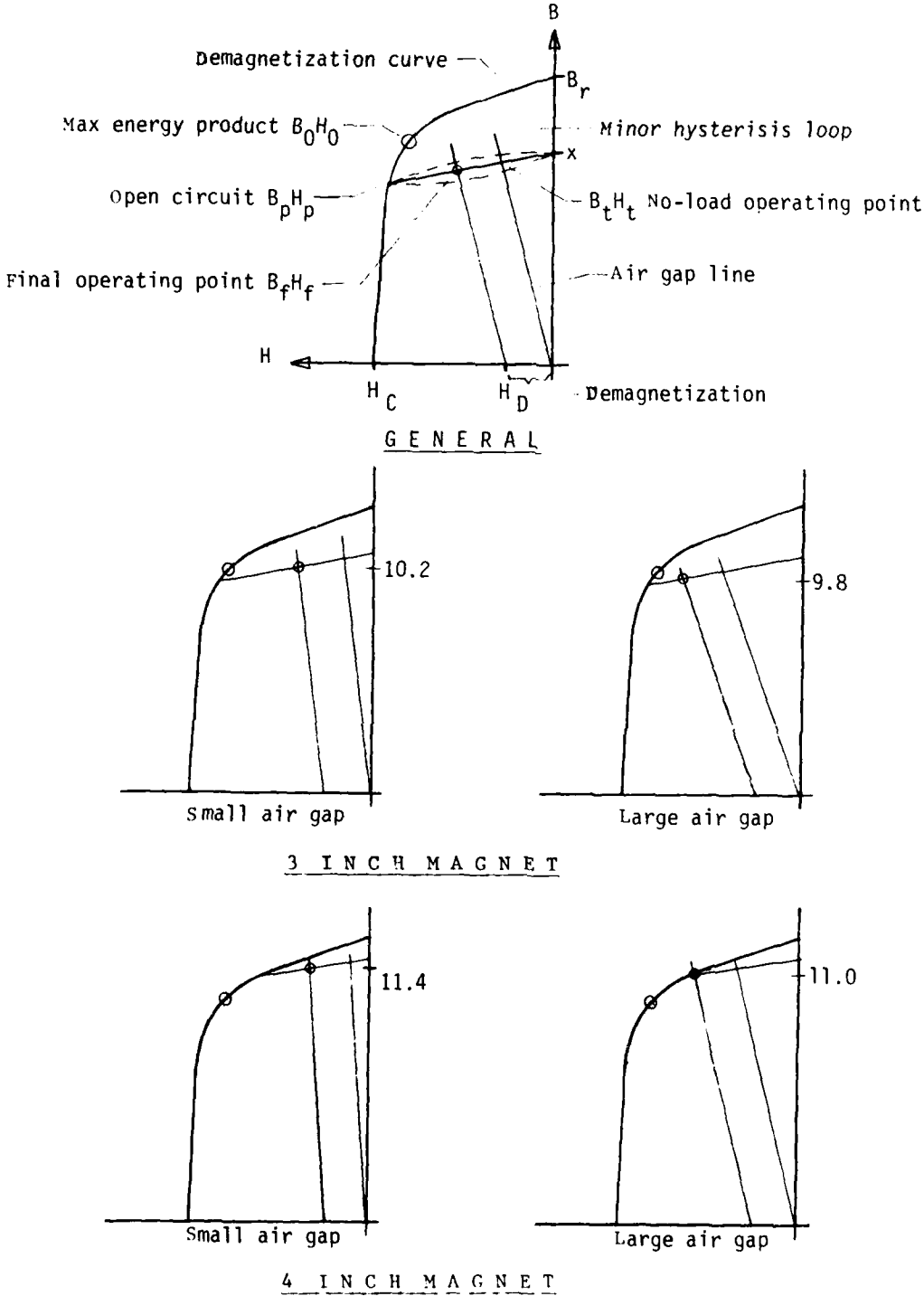

Figure 6. Flux variation with air gap and magnet length

Conversely, using a single pulse eliminates half of the circuit elements (one capacitor and one diode) and replaces them with the additional turns of hard wire which is less prone to failure. By locating the magnet at the end of the stroke, the carrier reverses direction before the negative pulse is generated. The result is that a single positive pulse is generated on the firing stroke and a single negative pulse on the recoil. The high demagnetizing effect of the recoil stroke is eliminated by the remaining diode in the circuit and the inertial switch is obviated.

Given ample space for the coil, the single pulse approach is preferable. The calculations, and to some extent the testing, did not account for the acceleration of the carrier. The number of turns predicted for the double-pulse approach is therefore likely to be low since the magnet enters the coil immediately on release of the sear. For the single pulse it enters later in the stroke when full speed has been achieved and the prediction should be more accurate.

Circuit Design

The voltage doubler circuit (fig. 7) is used to combine the energy of two pulses of opposite polarity. Each 80-volt pulse charges one of the two microfarad capacitors individually in the course of a stroke. Upon impact of the charged firing pin with the primer both capacitors are discharged in series to initiate the primer at 160 V. On the recoil stroke the acceleration of the carrier opens the inertial switch, S, and disconnects the circuit from the 250 volts generated at the coil thus preventing demagnetization. To enhance safety, a bleed resistor, R_b, discharges the circuit when the bolt carrier comes to rest in the charged position.

The circuit for a single pulse configuration is shown in figure 8. The diode allows only the low positive voltage generated on the firing stroke to charge the capacitor and isolates the high negative voltage of the recoil.

No attempt was made to optimize the electronic circuit for this study. Components should be selected to reliably withstand the physical and electrical environments of the gun over its expected serviceable lifetime.

Test Fixture

The test fixture used in this investigation (fig. 9) operates opposite to that of the gun by moving a simulated receiver tube containing the magnet through a stationary coil. The driving force is provided by an air cylinder. The velocity is a function of the pressure applied and is measured by a magnetic sensor on the tube. The circuit is mounted to the chassis. To test an actual primer, a cartridge holder and noise muffler are attached in line with the tube. A firing pin on the end of the tube impacts the primer immediately after charging the circuit as it would in the actual gun. Limitations of the fixture are its stroke, which is less than that of the gun, and its single cycle. The generator yoke was designed with a sliding end to accommodate magnets and coils ranging in

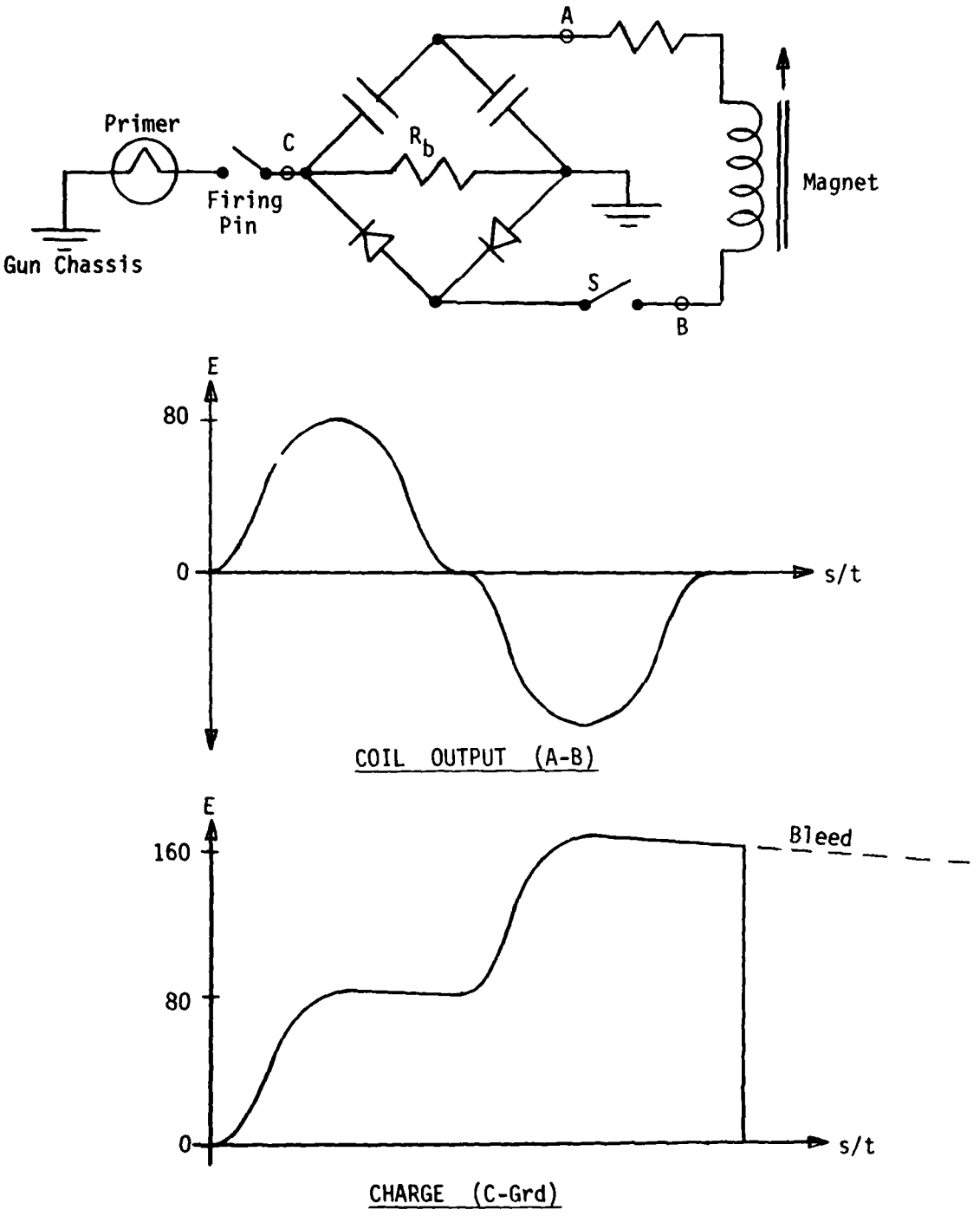

Figure 7. Bipolar pulse storage

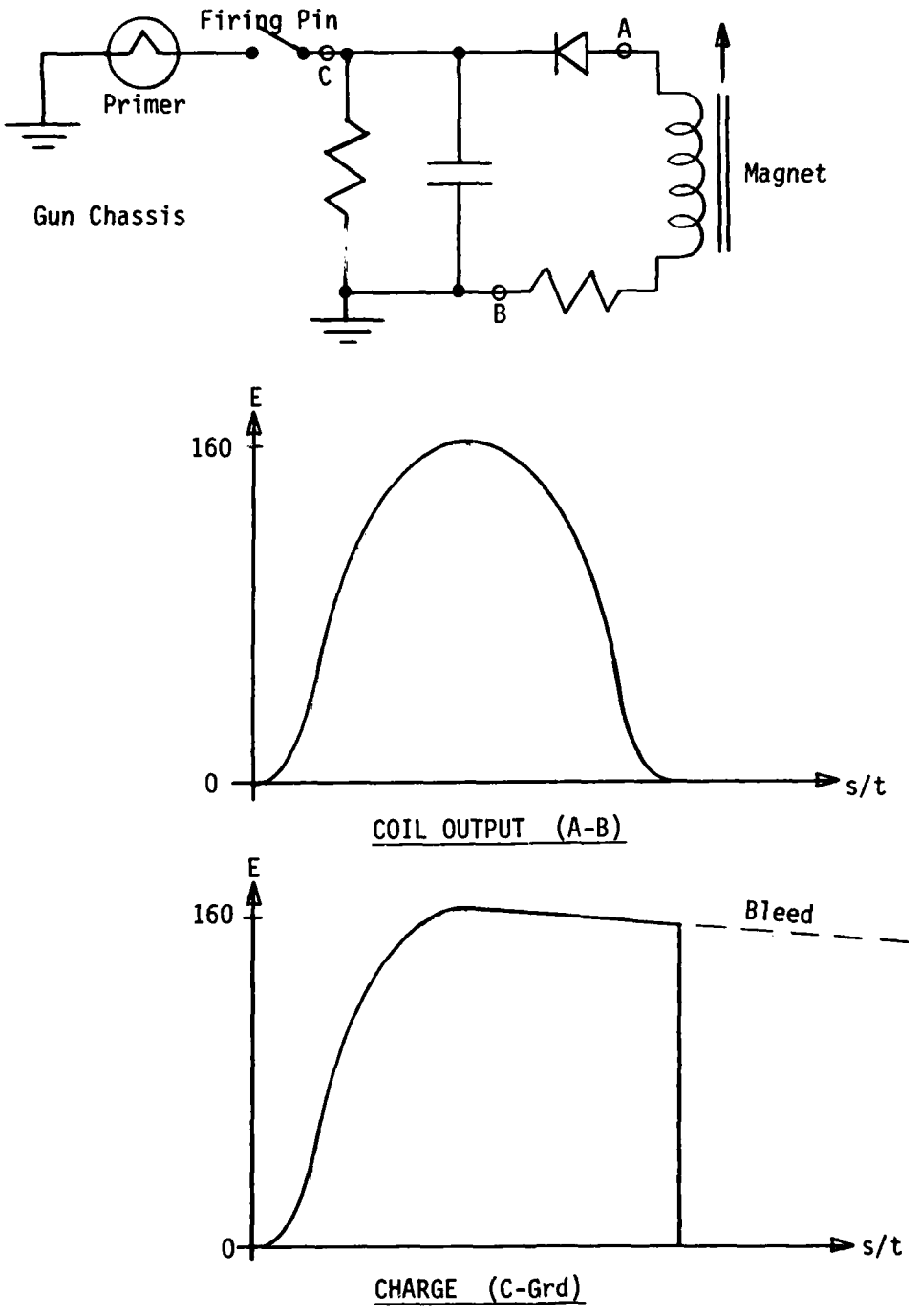

Figure 8. Single pulse voltage storage

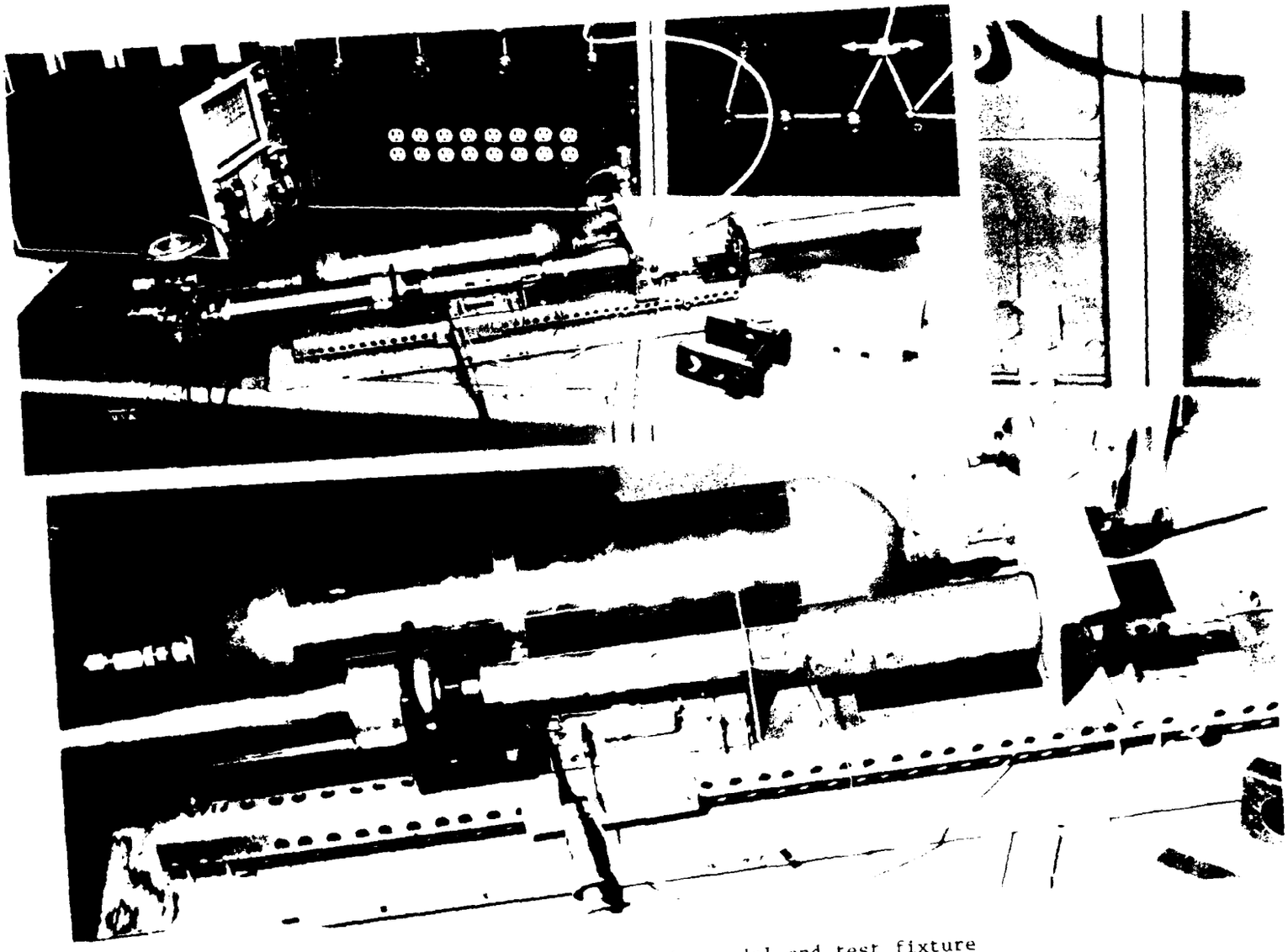

Figure 9. Demonstration model and test fixture

size from 3 to 4 inches. An 8000 turn coil 3-inches long was tested with 3- and 4-inch magnets with variations in the assembled configuration. A horseshoe-shaped yoke was also used which could accommodate the same magnets and two different magnetic path lengths.

The circuit consisted of two 4-microfarad tantalum capacitors, two 1N3253 diodes, and one 0.47M ohm bleed resistor. No. 34 AWG triple nylese wire, with a total resistance of 747 ohms was used for the coil.

TEST RESULTS

The tests performed in this study were intended to determine general characteristics and suitability of the design approach and the effects of variations in configuration. The limitations of the test fixture and availability of equipment precluded accumulation of precise data. However, the approximate values obtained are sufficient for comparison and selection of a second generation design.

Several variations in wave shapes were obtained (fig. 10) with the most significant differences resulting from the air gap.

The concentric yoke with a small (0.30 in.) air gap produced an almost square wave (fig. 10a) with a rapid rise time and a voltage spike at either end. Under open circuit, the trailing spike is generally 10% higher than the main pulse, but with the capacitor circuit connected it is more or less equal. In some cases, when it was higher, its duration was sufficient to charge the capacitor to the higher value. The size of the spike was also affected by cutting a longitudinal slot in the receiver tube (aluminum) to reduce eddy current resistance in the tube. With an 8000-turn coil, the amplitude of the main pulse reached 80 volts. This is in reasonable agreement with the calculated value.

Increasing the air gap to 0.250 in. changes the wave to a sinusoidal shape (fig. 10b). There is less than 10% reduction in peak voltage, but a marked decrease in the magnetic drag, as the magnet poles pass adjacent to the yoke.

Removal of the entire yoke resulted in a 15% decrease in peak amplitude and produced a pulse shape identical to that of a large gap.

A horseshoe yoke produces a triangular or trapezoidal wave. The combination of elements used for the test inadvertently resulted in a resonant condition which caused the output to exceed the expected value. The pulse shown in figure 10c peaks at 84 volts in contrast to the 80 volts from the concentric configuration described above. If, however, there is any remaining charge in the capacitors the tuning is upset and the output is reduced to 72 volts in the form shown in figure 10d. Shortening the magnetic path through the yoke, which brings the coil closer to the magnet itself, raises both these peak voltages. In general, because of the increased path length, the horseshoe yoke produced a slightly lower output than the concentric yoke. It may be possible to tune the concentric yoke to behave in the same manner, but this phenomenon requires means to assure an uncharged condition at all times prior to each firing stroke.

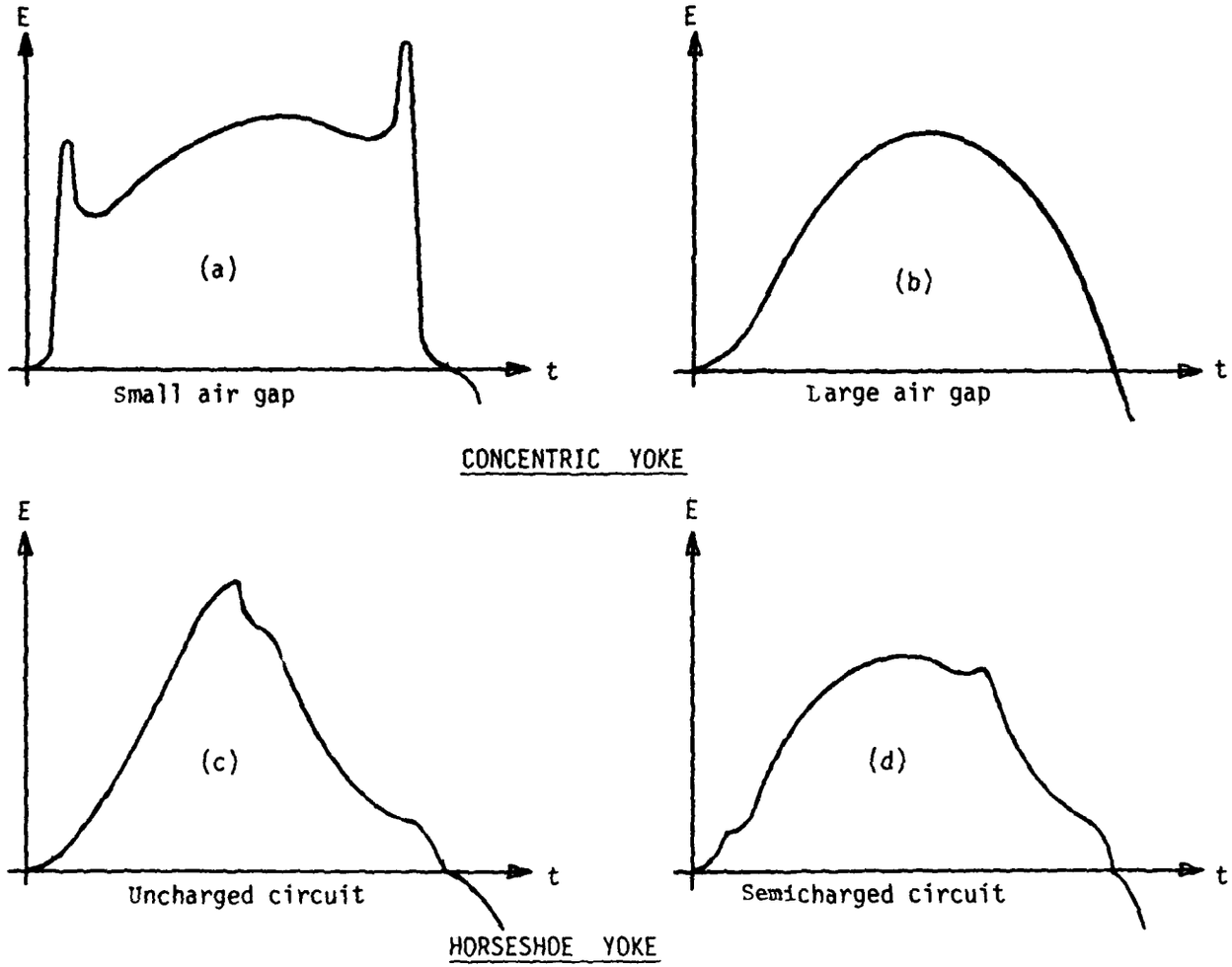

Figure 10. Voltage output wave shape variations

An unexplained anomaly occurred occasionally with the voltage doubler circuit. Shortly after reaching full charge, the combined voltage level of the circuit dropped to an intermediate level. In several instances this drop occurred later than the time at which the primer would have been initiated.

Tests were performed using actual M52 electric primer. Using the concentric yoke with a 3-in. magnet and small air gap, 15 primers were successfully initiated on the first attempt.

APPLICATION

There are two possible locations for the coil, each requiring modest modification to the gun: (1) around the upper receiver tube between the rear bolt carrier yoke and the buffer retainer in the concentric design and (2) around the rear of the bolt carrier tube in the horseshoe design. In the first design, the dust cover must be enlarged to clear the coil yoke. For the second design, the rear bolt carrier yoke must be removable in order to replace the coil, but the dust cover and related parts remain unchanged. In both cases the buffers must be relocated, probably to the back plate between the grips.

The firing pin becomes charged with the capacitor and must be insulated. The entire pin may have an insulated covering, or an insulated point may be connected to a rear hot shoe by a conductor interior to the pin (i.e., an insulated wire in a slot). The latter avoids interference with the retaining pin and the cam pin. In both, the bolt must be adequately insulated where the pin passes through to avoid arcing.

Electrical connections among the various elements of the firing device must be arranged to facilitate disassembly and replacement of components. Such connections should be rugged enough to withstand rough handling yet insure reliability. Connection of the circuit components to the coil is most critical. Ideally, they should be packaged together with permanent connections to assure that all of the energy generated is captured. The timing of the discharge (firing) is not as critical and contact bounce at this connection is more tolerable.

Two applications of a firing device to the gun are illustrated in figures 11 and 12. The concentric design with a contact spring projecting through the bolt carrier tube to connect to the firing pin is shown in figure 11. Coil size is maximized by extending it into the rear yoke and using it to carry the magnetic flux. The circuit elements are housed in a protruding case at the top. If the diameter of the coil was decreased, this space would be too small for a single capacitor. Consideration should then be given to combining several smaller capacitors, packaging them adjacent to the coil, or procuring a special doughnut shaped capacitor designed to fill the entire annulus. A coil of the scale shown can easily accommodate the turns required for a single-pulse approach.

A horseshoe configuration is shown in figure 12. The coil in this approach fits around the carrier tube and uses it, the rear yoke, and an additional yoke (in lieu of the buffer retainer) to carry the magnetic flux. Circuit elements are packaged in an extension of the coil case beneath the carrier. Since the case would very likely be molded plastic, a negative contact is required. The

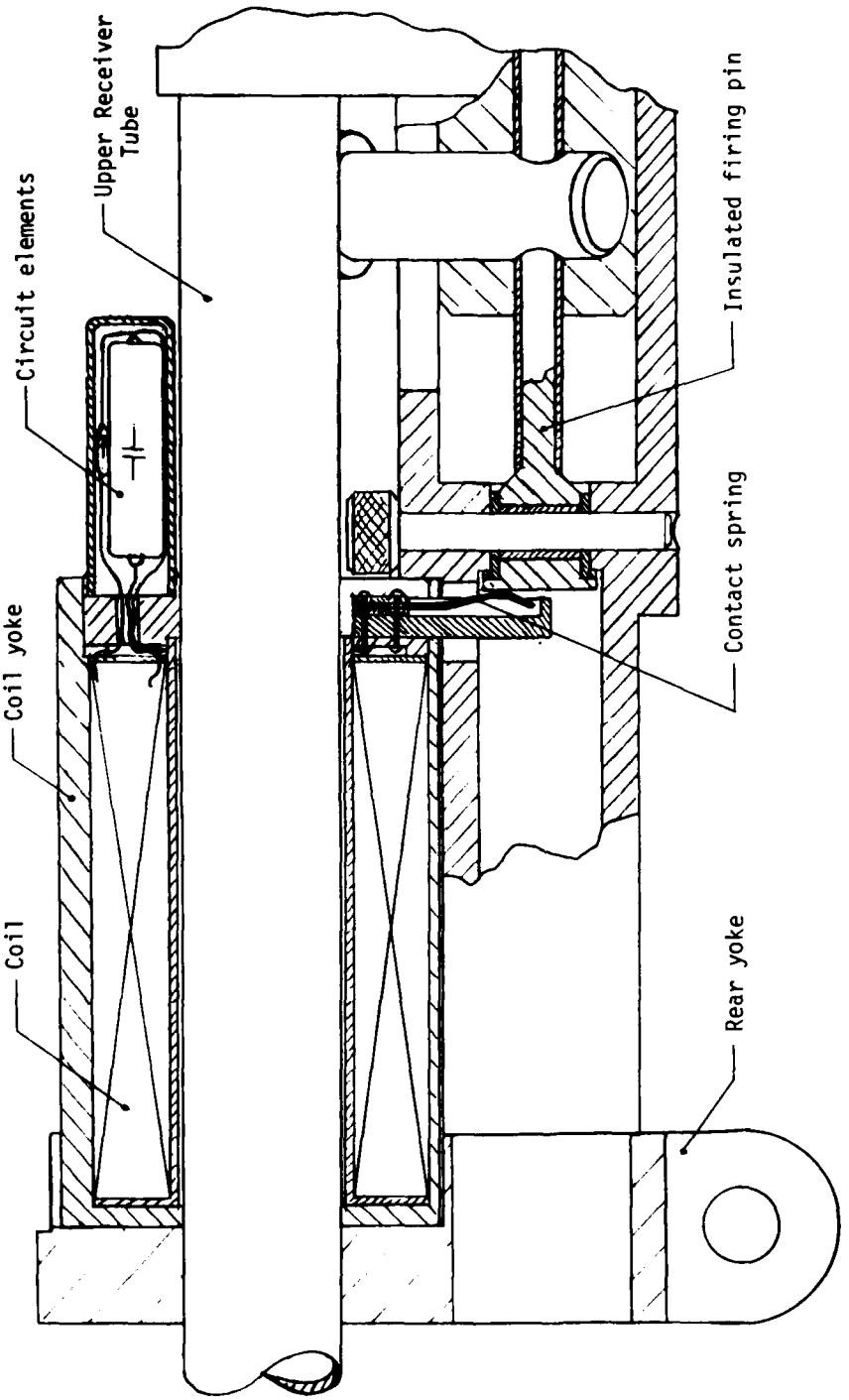

Figure 11. Firing device - carrier assembly

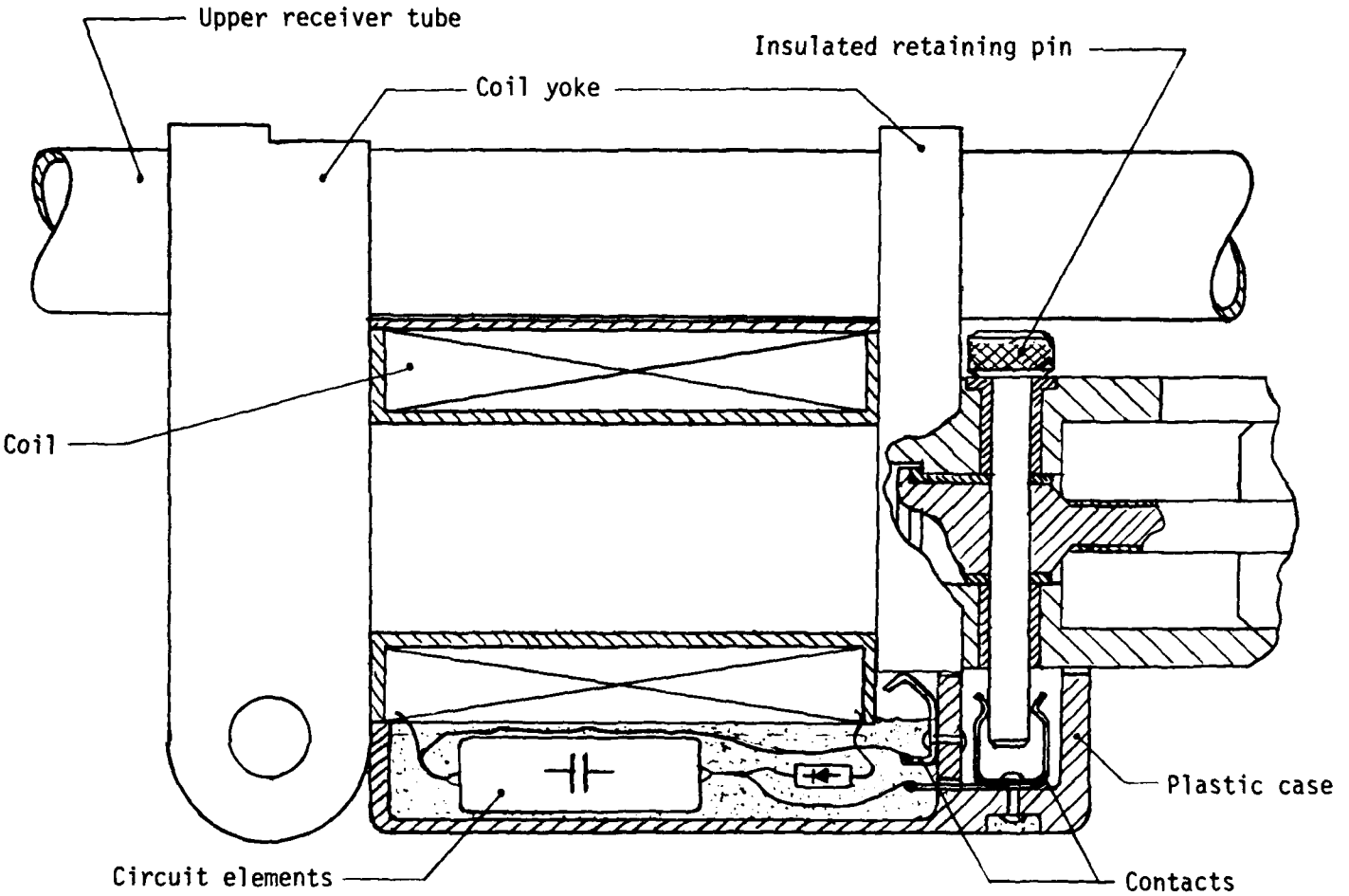

Figure 12. Horseshoe firing device - carrier assembly

firing device output reaches the firing pin through an insulated retaining pin. A tight fit is not required here since upon impact electrical contact is assured.

An alternative location for the circuit elements is within the carrier tube behind the firing pin. Since the removable connection is on the charging side, its design requires more care.

Other 20-mm firing pins have been successfully insulated with Plastic; L-P-385, Type 1, Class 3.

CONCLUSIONS

1. Using the kinetic energy of the operating group assembly, it is feasible to generate electric power sufficient to initiate electric primed 20-mm ammunition.

2. The design can be implemented without the use of exotic materials, unusual tolerancing, or major revisions to the current gun design concept.

3. A second-generation model built into a functional weapon is necessary to obtain more representative data and establish the appropriate design parameters.

4. The single-pulse design, in spite of its larger size, appears to have the most merit at this time.

5. Special emphasis should be placed on the selection of reliable electronic components appropriate to this application.

APPENDIX

CALCULATIONS

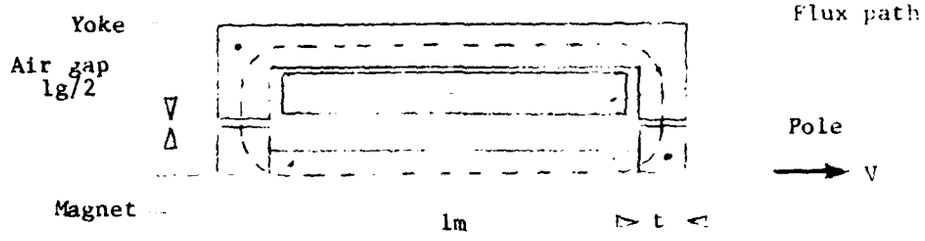

Area of Magnet $Am = 0.44 \text{ in.}^2 = 2.85 \text{ cm}^2$

Gap Length $lg = 0.03 \text{ in.} = 0.076 \text{ cm}$

Pole Width $t = 0.50 \text{ in.} = 1.27 \text{ cm}$

Diameter of Magnet $Dm = 0.75 \text{ in.} = 1.91 \text{ cm}$

Length of Magnet $lm = 3.00 \text{ in.} = 7.62 \text{ cm}$

Magnet Material: Cast ALNICO $\underline{\underline{V}}$

$B_r = 12{,}400$ gauss

$H_C = 640$ oersteds

$B_0 = 10{,}000$ gauss

$H_0 = 530$ oersteds

$B_0H_0 = 5.3\ (10^6)$

For an open circuited magnet:

$$B/H = (1.89 - a)\ (lm/D + a)^{1.82}$$

for ALNICO $\underline{\underline{V}}$ $\quad a = 0.901\ \left(2\,\frac{B_rH_C}{B_0H_0} - \frac{B_rH_C}{B_0H_0}\right)$

$$B/H\ (1.89 - 0.901)\ \left(\frac{7.62}{1.91} + 0.901\right)^{1.82} = 17.85$$

From demagnetization curve:

$B_p = 9600\ G$, $H_p = 550$ Oe

$B_pH_p = 5.28\ (10^6) \approx B_0H_0$ (max energy product)

OPERATING POINTS:

(Intersection of minor hysterisis loop with air gap line.)

$$B_t = \frac{B_p - mH_p}{1 - \frac{mf\ Am\ lg}{F\ Ag\ lm}} \quad ; \quad H_t = \frac{B_p - mH_p}{\frac{f\ Am\ lg}{F\ Ag\ lm} - m}$$

Slope of minor hyst loop:

$$m = -\frac{B_r}{H_C}(1-a) = -\frac{12400}{640}(1-0.901) = -1.92$$

Negligible leakage flux links coil at start

$$\therefore f = F = 1$$

Considering fringing for $A_{yoke} > A_{magnet}$:

$$Ag = \frac{\pi}{4}(D + 2l_g)^2 = \frac{\pi}{4}[0.75 + 2(0.03)]^2 = 0.52 \text{ in.}^2 = 3.32 \text{ cm}^2$$

$$B_p - mH_p = 9600 + 1.92\ (550) = 10{,}656 \text{ G}$$

$$B_t = \frac{10{,}656}{1 + \frac{1.92\ (2.85)\ (0.076)}{(3.32)\ (7.62)}} = \frac{10{,}656}{1 + 1.92\ (0.00856)} = \begin{cases} 10{,}483 \text{ G} \\ 1.05 \text{ Web/m}^2 \end{cases}$$

$$H_t = \frac{10{,}656}{\frac{1}{0.00856} + 1.92} = \begin{cases} 90 \text{ Oe} \\ 7141 \text{ A/m}^2 \end{cases}$$

FLUX IN GAP:

$$B_t/_{GAP} = B_t/_{MAG}\left(\frac{Am}{Ag}\right) = 10{,}483\left(\frac{2.85}{3.32}\right) = \begin{cases} 9000 \text{ G} \\ 0.9 \text{ Web/m}^2 \end{cases}$$

$$\phi_g = B_g A_g = (0.9)\ (3.32)\ (10^{-4}) = 3 \times 10^{-4} \text{ Webers}$$

VOLTAGE GENERATION:

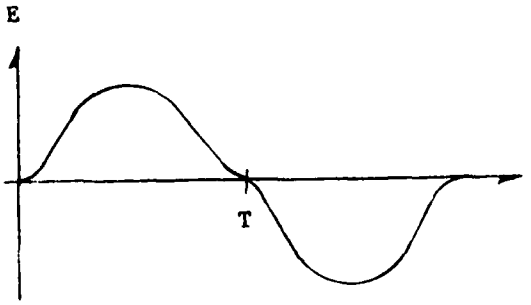

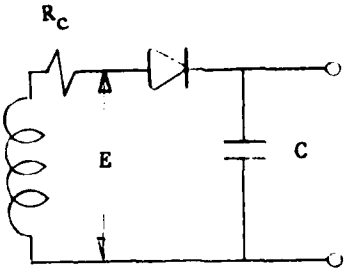

Magnet Velocity $V = 110$ in./sec

Desired Peak Voltage $E = 160$ volts (use 170)

Pulse Duration $T = l_m/V = \frac{3}{110} = 0.027$ sec

$$N = \frac{ET}{\phi} = \frac{170\ (0.027)}{3\ (10^{-4})} = 15{,}300 \text{ turns}$$

(for open circuit condition)

For full charge: $T \geq 5RC$

$$R_{MAX} = \frac{T}{RC} = \frac{0.027}{5\ (2)\ (10^{-6})} = 2700\ \Omega$$

COIL SIZING

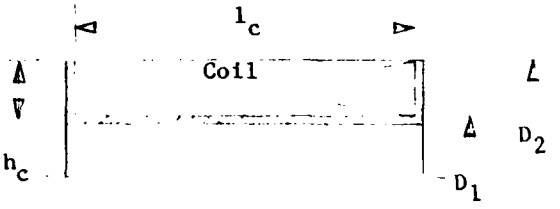

d_w = wire dia.

stack factor = 0.933

$$N_{MAX} = \frac{h_c l_c}{0.933\ d_w^2} = \frac{(D_2 - D_1) l_c}{1.866\ d_w^2}$$

$$D_2 = D_1 + (1.866)\ \frac{d_w^2 N}{l_c}$$

Total wire length: $L_w = \pi\ (\frac{D_2 + D_1}{2})N$

Coil Resistance: $R_c = 1.57\ (D_1 + D_2)\ N\ (\frac{R'}{12})$

$$= 0.131\ (D_1 + D_2)\ NR'$$

R' = wire res/M ft

For 15,300 turns of AWG 32 wire (d = 0.0108 in.):

$$D_2 = 1.1 + 1.866 \left[\frac{(0.0108)^2(15{,}300)}{3}\right] = 2.2 \text{ in. (don't fit)}$$

With AWG 34 wire (d = 0.0078, $R' = 0.260$):

$$D_2 = 1.1 + 1.866 \left[\frac{(0.0078)^2(15{,}300)}{3}\right] = 1.67 \text{ in.}$$

$$R_c = 0.131\ (1.1 + 1.67)\ (15{,}300)\ (0.260) = 1444\ \Omega < R_{MAX}$$

DEMAGNETIZATION:

$$H_d = \frac{NI}{l_m} = \frac{NE}{Rl_m} = \frac{(15{,}300)\ (170)}{1444\ (0.0762)} = \begin{cases} 23{,}638 \text{ A/m} \\ 297 \text{ Oe} \end{cases}$$

from demagnetization curve: $B_t = 9900$ G

Final air gap flux:

$$\phi_g = B_t A_m = 0.99\ (2.85)\ (10^{-4}) = 2.82\ (10^{-4}) \text{ Web}$$

Adjusted Voltage:

$$E = \frac{N\phi}{T} = \frac{15{,}300\ (2.82)}{0.027\ (10^4)} = 160 \text{ volts}$$

Using both pulses and voltage doubler circuit:

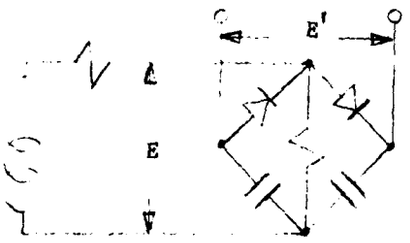

E = 80 V (use 85)

$$N = \frac{ET}{\phi} = 7650 \text{ turns}$$

$$D_2 = 1.1 + 1.866 \left[\frac{(0.0078)^2(7650)}{3}\right] = 1.39 \text{ in.}$$

$$R_c = 0.131\ (1.1 + 1.39)\ (7650)\ (0.260) = 648\ \Omega$$

$$I = E/R = \frac{85}{648} = 0.131 \text{ Amp}$$

$$H_d = \frac{NI}{l_m} = \frac{7650\ (0.131)}{0.0762} = \begin{cases} 13{,}155\ \text{A/m} \\ 165\ \text{Oe} \end{cases}$$

B_r drops to 10,150 G

Final Air Gap Glux:

$$\phi_g = B_t A_m = 1.015\ (2.85)\ (10^{-4}) = 2.9\ (10^{-4})\ \text{Web}$$

$$E = \frac{N\phi}{T} = \frac{7650\ (2.9)}{(0.027)\ (10^4)} = 82\ \text{V}$$

RECOIL:

For V_R = 300 in./sec:

$$T = l_m/V_R = \frac{3}{300} = 0.010\ \text{sec}$$

$$E = \frac{N\phi}{T} = \frac{15{,}300\ (3)\ (10^{-4})}{0.010} = 459\ \text{volts}$$

For bipolar pulse: E = 230 volts

$$H_d/_{\text{single}} = \frac{NE}{Rl_m} = \frac{15{,}300\ (459)}{1444\ (0.0762)} = \begin{cases} 63{,}823\ \text{A/m} \\ 802\ \text{Oe} \end{cases} > H_c$$

$$H_d/_{\text{bipolar}} = \frac{7600\ (230)}{648\ (0.0762)} = \begin{cases} 35{,}400\ \text{A/m} \\ 445\ \text{Oe} \end{cases}$$

B_f = 9600 G for small air gap

no demagnetization but marginal

DISTRIBUTION LIST

Administrator
Defense Technical Information Center
ATTN: Accessions Division (12)
Cameron Station
Alexandria, VA 22314

Office of the Deputy
Undersecretary of Defense
Research and Engineering
Pentagon Room, 3D1098
ATTN: Mr. R. Thorkildson
Washington, DC 20301

Commander
U.S. Army Materiel Development
and Readiness Command
ATTN: DRCDE-DH
DRCDE-DA
DRCDE-DG
DRCIRD
5001 Eisenhower Avenue
Alexandria, VA 22333

Commander
Combined Arms Center
ATTN: ATCA-COF
Ft. Leavenworth, KS 66048

Commander
U.S. Army Training and
Doctrine Command
ATTN: Library Bldg 133
Ft. Monroe, VA 23651

Director
U.S. Army TRADOC Systems
Analysis Activity
ATTN: ATAA-SL
White Sands Missile Range, NM 88002

Commander
U.S. Army Missile Research and
Development Command
ATTN: DRSMI-AOM
RDDMI-R
Redstone Arsenal, AL 35809

Commander
U.S. Army Air Defense School
ATTN: Technical Library
P.O. Box 5040
Ft. Bliss, TX 79916

Assistant Commandant
U.S. Army Armor School
ATTN: Technical Library
Ft. Knox, KY 40121

Commandant
U.S. Army Field Artillery School
ATTN: Morris Swett Library
Ft. Sill, OK 73503

Commander
U.S. Army Tank-Automotive Research
and Development Command
ATTN: DRDTA-UL, Library
Warren, MI 48090

Commandant
U.S. Army Aviation Center
ATTN: USAAVNT, Library
P.O. Box 0
Ft. Rucker, AL 36362

Director
U.S. Army Materiel Systems
Analysis Activity
ATTN: DRXSY-D
DRXSY-MP
Aberdeen Proving Ground, MD 21005

Commander
U.S. Army Communications Research
and Development Command
ATTN: DRDCO-SGS
Ft. Monmouth, NJ 07703

Commander
Harry Diamond Laboratory
ATTN: DELHD-PP
2800 Powder Mill Road
Adelphi, MD 20783

Commander
U.S. Army Electronics Research
and Development Command
Technical Support Activity
ATTN: DELSD-L
Ft. Monmouth, NJ 07703

Commander
U.S. Army Aviation Research
and Development Command
ATTN: DRDAV-EVW
P.O. Box 209
St. Louis, MO 63166

Program Manager
Fighting Vehicle Systems
MAMP Bldg 1
ATTN: DRCPM-FVS-SEA
Warren, MI 48090

Project Manager, Advanced Attack Helicopter
Product Manager for 30-mm Ammunition
ATTN: DRCPM-AAH-30-mm
Dover, NJ 07801

Project Manager
DIVAD Gun
ATTN: DRCPM-ADG
Dover, NJ 07801

Project Manager
Advanced Attack Helicopter
ATTN: DRCPM-AAH
P.O. Box 209
St. Louis, MO 63166

Commander
U.S. Army Armament Materiel
Readiness Command
ATTN: DRSAR-LE
DRSAR-LEI
DRSAR-LED
DRSAR-LEA
DRSAR-LEP-L
Rock Island, IL 61299

Headquarters
U.S. Army Research and
Technical Laboratory
AMES Research Center
ATTN: DAVDL-AS
Moffett Field, CA 94035

Chief
Benet Weapons Laboratory, LCWSL
U.S. Army Armament Research
and Development Command
ATTN: DRDAR-LCB-TL
Watervliet, NY 12189

Commander
U.S. Army Armament Research
and Development Command
ATTN: DRDAR-BL-TD
Aberdeen Proving Ground, MD 21005

Commander/Director
Chemical Systems Laboratory
U.S. Army Armament Research
and Development Command
ATTN: DRDAR-CLJ-L
DRDAR-CLB-PA
APG, Edgewood Area, MD 21010

Commander
Naval Weapons Center
ATTN: Code 3176
China Lake, CA 93555

Commander
Naval Ordnance Station
ATTN: Code 50211
Louisville, KY 40219

Department of the Navy
Naval Air Systems Command
ATTN: Code 5323D
Washington, DC 20361

Commander
Naval Surface Weapons Center
ATTN: Mr. C. Samuels (Code G22)
Mr. Childeics (Code C051)
Dahlgren, VA 22448

Commander
Air Force Armament Laboratory
ATTN: ADTC-SD-20
AFATL-DLDG
AFATL-DLD
AFATL-DLDA
AFATL-DLDL
Eglin Air Force Base, FL 32548

Deputy for A-10
ATTN: ASD-YXA
Wright Patterson, OH 45433

Commander
U.S. Army Armament Research
and Development Command Test Site
Brindle Lake, Ft. Dix
Ft. Dix, NJ 08640

Director
Ballistic Research Laboratory
U.S. Army Armament Research
and Development Command
ATTN: DRDAR-TSB-S
Aberdeen Proving Ground, MD 21005

Commander
Naval Weapons Support Center
ATTN: Code 7042
Crane, IN 47522

Commandant
U.S. Coast Guard
ATTN: G-OMR/74
Washington, DC 20591

Commander
U.S. Army Armament Research
and Development Command
ATTN: DRDAR-TSS (5)
DRDAR-SA
DRDAR-SCA (10)
DRDAR-SEI
DRDAR-LMC
DRDAR-LCN
DRDAR-LCN-C (2)
AFTE-LO-AC
Dover, NJ 07801

ED

8